Available online at www.sciencedirect.com
SCIENCE DIRECT®
Journal of Catalysis 227 (2004) 53–59
JOURNAL OF CATALYSIS
www.elsevier.com/locate/jcat

Oscillation in low-temperature NO–H_2–O_2 reactions over Pt catalysts supported on NO_x-adsorbing material, TiO_2–ZrO_2

M. Machida *, S. Ikeda

Department of Applied Chemistry and Biochemistry, Faculty of Engineering, Kumamoto University, 2-39-1 Kurokami, Kumamoto 860-8555, Japan

Received 29 May 2004; revised 20 June 2004; accepted 22 June 2004

Available online 20 July 2004

Abstract

The oscillatory behavior of 0.08% NO–0.28% H_2–10% O_2 reactions in a flowing He ($W/F = 0.24\ s\,g\,cm^{-3}$) over 1 wt% Pt/$TiO_2$–$ZrO_2$ catalyst has been studied at 90 °C with attention to the NO_x adsorption property of the support oxide. After an induction period of ca. 20 h in a steady-state flow, oscillations appeared with different periods and amplitudes depending on the concentration of H_2 in the gas feed. During the oscillation, the conversions of both NO and H_2 were decreased simultaneously from the steady state, whereas the corresponding N_2/N_2O yields were more than estimated from the reaction stoichiometry. The parallel TPD measurement revealed that the amount of nitrate (NO_3) accumulation on the catalyst became largest when the oscillation started. In situ DRIFTS detected two different nitrates species with unidentate and bidentate structures, which adsorbed on basic sites forming at the boundary of two oxide components. Based on the fact that the surface coverage of nitrate on the support is correlated to the oscillation period, a mechanism is suggested in which the surface domains of accumulated nitrates block the adsorption of gaseous NO, leading to a sudden drop of the catalytic activity. However, with the progress of nitrate removal by the reaction with H_2, the adsorption of NO onto Pt can restart the catalytic NO reduction.

Keywords: Oscillation; NO–H_2–O_2 reaction; Platinum; TiO_2–ZrO_2; Oxidative NO adsorption

1. Introduction

Recently, increasing attention has been paid to the NO reduction by H_2 in an excess O_2 (NO–H_2–O_2 reaction) at low temperatures of $\leqslant 150$ °C [1–10]. Platinum is the most effective catalyst for this purpose, but the activity is dependent on support materials [9]. Although acidic and/or amphoteric oxides (SiO_2, ZrO_2, Al_2O_3, Y-zeolite, ZSM-5, SiO_2–Al_2O_3, etc.) are rather effective support materials, considerably more N_2O than N_2 is produced. By contrast, the activity of Pt becomes very low by the use of oxides with high basicity (CeO_2 and La_2O_3) or transition metal oxides having redox properties (Mn_2O_3, NiO, and CuO). The NO–H_2–O_2 activity of Pt catalysts may therefore be explained on the basis of the acidic/basic character of support materials.

We have previously reported that Pt supported on porous TiO_2–ZrO_2 exhibits higher NO conversion to N_2 in the stream of 0.08% NO–0.28% H_2–10% O_2–He balance at $\leqslant 100$ °C [6,10]. This amorphous binary oxide is known to create Lewis acid as well as basic sites at the boundary of two components in a porous framework [11,12]. Due to the presence of basic sites, a large amount of NO (ca. 0.4 $mmol\,g^{-1}$ at 90 °C) adsorbs oxidatively to yield nitrate species (NO_3), which monopolize the Pt surface and thus suppress the competitive occurrence of H_2–O_2 reactions thereon. This is the reason why nearly stoichiometric nitrate–H_2 reactions take place at < 100 °C even in an excess O_2. The interaction between oxidative NO adsorption and simultaneous catalytic NO–H_2–O_2 reaction is expected to cause a characteristic feature, which cannot be seen in other catalyst systems.

* Corresponding author. Fax: +81 96 342 3651.
E-mail address: machida@chem.kumamoto-u.ac.jp (M. Machida).

0021-9517/$ – see front matter
doi:10.1016/j.jcat.2004.06.019

In the present work, we have found the occurrence of catalytic oscillations in the NO–H_2–O_2 reaction over Pt/TiO_2–ZrO_2 as a result of the accumulation of oxidatively adsorbed NO_x after a long induction period. The oscillation behavior is well known for many catalytic reactions including H_2–O_2, CO–O_2, CH_4–O_2, over several noble metal catalysts under specific conditions [13]. Increased interest has especially been aroused on oscillatory phenomena in the catalytic conversions of NO [14,15] and N_2O [16,17], where surface oxygen plays a key role as in the case of the catalytic oxidation. Oscillation in the NO–CH_4–O_2 reaction over Pd/TiO_2 is the result of periodic phase changes between Pd and PdO, which are accompanied by temperature oscillations [14]. Two other mechanisms were proposed for the NO–C_2H_4–O_2 reaction over Pt–ZSM-5 [15], i.e., the kinetic inhibition effect of NO on the catalytic surface and the surface phase transition of Pt induced by adsorbed NO. For NO–H_2 reactions, oscillation have only been observed on single-crystal Pt, Rh, and Ir surfaces under low pressures in a range 10^{-6}–10^{-5} mbar at temperatures between 400 and 500 K [18,19]. This is explained by a vacancy mechanism, where oscillations occur between an absobate-free and O + NO covered surface. However, the oscillating catalytic NO–H_2 reaction in excess O_2 under atmospheric conditions is not well known.

The oscillatory behavior during the NO–H_2–O_2 reaction over a Pt/TiO_2–ZrO_2 catalyst was studied under steady-state gas feed conditions in the presence of a large excess O_2. We present experimental evidence based on quantitative analysis of products during oscillation, in conjunction with TPD and in situ DRIFTS measurement, that the oscillation occurs as a result of accumulation of oxidatively adsorbed NO_x. The mechanism for the catalytic oscillation is discussed from viewpoints of the NO_x adsorbability of the support material as well as the catalytic property of Pt.

2. Experimental

2.1. Catalyst preparation and characterization

The equimolar binary oxide, TiO_2–ZrO_2, was prepared by precipitation from $Ti(OPr)_4$/$ZrO(NO_3)_2$ mixtures by adding aqueous ammonia and subsequent evaporation to dryness. The resultant solid product was calcined at 450 °C in air. The other support oxides, γ-Al_2O_3 (JRC-ALO-4) and SiO_2 (JRC-SIO-5), which were supplied by the Catalysis Society of Japan, were used as a reference. These oxides were impregnated with an aqueous solution of hydrogen hexachloroplatinate (IV) and then calcined at 450 °C to produce supported Pt catalysts (1 wt% loading). The catalysts were reduced in 5% H_2/He at 400 °C for 1 h prior to characterization and/or catalytic reactions. As prepared samples was confirmed to consist of a noncrystalline phase by powder X-ray diffraction (XRD, Rigaku Multiflex) using monochromated Cu$K\alpha$ radiation (30 kV, 20 mA). The BET surface area was obtained by measuring N_2 adsorption isotherms at −196 °C. The dispersion of Pt was determined by O_2–H_2 titration at room temperature [20].

2.2. In situ DRIFTS

In situ DRIFT spectra of NO_x species adsorbed on Pt/TiO_2–ZrO_2 were recorded on a Jasco FTIR-610 spectrometer. The sample was placed in a temperature-controllable diffuse reflectance reaction cell (Jasco DR600A), which was connected to a gas-flow system. The sample was first treated in a stream of 5% H_2/He at 400 °C for 1 h and next exposed to gas mixtures of 0.08% NO, 0.28% H_2, 10% O_2, and He balance at 90 °C for 2 h. This was followed by spectra measurement of NO_x adsorbates in a flowing He at the same temperature. The sample on exposure to the reaction mixture was next heated in a stream of He at elevated temperatures. Immediately following this treatment, the cell was cooled to 90 °C, where spectrum was measured. At a resolution of 4 cm^{-1}, 512 scans were usually recorded. All spectra thus obtained were transformed into absorption spectra by the use of the Kubelka–Munk function and referenced to those taken just before the admission of reaction mixtures.

2.3. Catalytic reactions

The steady-state catalytic NO–H_2–O_2 reaction was carried out in a conventional flow system at atmospheric pressure. Granular catalysts (10–20 mesh, 0.2 g) were fixed in a quartz tube (6 mm i.d.) by packing quartz wool at both ends of the catalyst bed, which was placed in a water-cooled infrared image furnace. Gas mixtures of 0.08% NO, 0.14–1.0% H_2, and 10% O_2 balanced with He were fed to the catalyst bed at $W/F = 0.24$ s g cm^{-3}. The effluent gas was analyzed by an on-line gas chromatograph (TCD) with a molecular 5A sieve and Porapak-Q columns, a chemiluminescence NO_x analyzer, and a quadrupole mass spectrometer. The uncertainty of NO_x concentration measured by a chemiluminescence NO_x analyzer is estimated to be within 2%. The conversion of NO_x was defined using the ratio of concentration at the inlet and outlet, $1 - ([NO] + [NO_2])_{outlet}/([NO] + [NO_2])_{inlet}$. The measurement of breakthrough curves for adsorptive NO removal was also carried out in the flow reactor. Granular sample (10–20 mesh, 0.2 g) was placed in a stream of 0.08% NO, 2% O_2 balanced with He ($W/F = 0.24$ s g cm^{-3}) at 90 °C with monitoring the NO_x concentration in the effluent gas.

3. Results

3.1. Oscillation in NO–H_2–O_2 reaction over Pt/TiO_2–ZrO_2

In a conventional fixed-bed reactor, self-sustained oscillatory NO–H_2–O_2 reactions were observed for 1 wt% Pt/TiO_2–ZrO_2 at 90 °C. Fig. 1 shows a profile of NO_x concentration at the reactor outlet during the steady feed of a gas

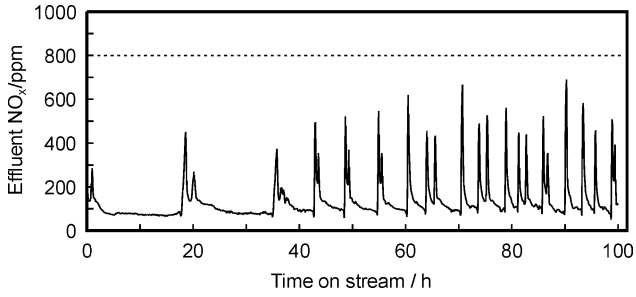

Fig. 1. Effluent NO_x concentration in NO–H_2–O_2 reaction over Pt/TiO_2–ZrO_2 at 90 °C. 0.08% NO, 0.28% H_2, 10% O_2, He balance, W/F = 0.24 s g cm^{-3}.

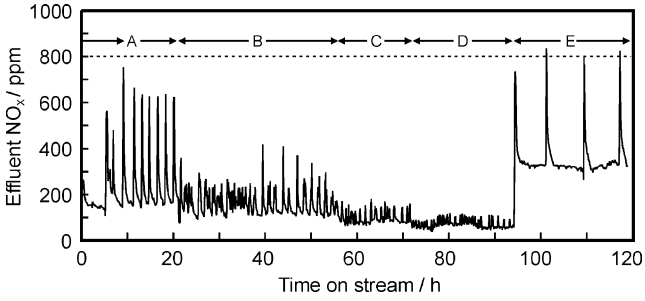

Fig. 2. Effect of H_2 concentration on oscillation of NO–H_2–O_2 reactions: A, 0.28%; B, 0.56%; C, 0.84%; D, 1.00%; E, 0.14%, 0.08% NO; 10% O_2, He balance, W/F = 0.24 g s cm^{-3}.

mixture of 0.08% NO, 0.28% H_2, 10% O_2, and He balance for 100 h. The catalytic reaction almost reached the steady state during the initial 18 h. Soon after this induction period, however, the effluent NO_x concentration began to oscillate temporarily, giving rise to a couple of sharp peaks. After the second fluctuation occurred at ca. 35 h, more frequent oscillatory behavior was observed. During the oscillations, the temperature fluctuation at the catalyst bed was less than ±1 °C.

The effects of hydrogen on the oscillatory behavior were studied by changing the H_2 concentration in the gas feed from 0.14 to 1.0% with keeping NO and O_2 concentrations constant. The oscillation occurred in every case, but the induction period became longer with increasing H_2 concentration. Fig. 2 shows the resultant profile of NO_x concentration in the effluent after an induction period. Here, the level of baseline corresponded to the steady-state conversion of NO, which was increased with an increase of H_2. The dependence of oscillation behavior on H_2 concentration can be summarized as follows: (i) the oscillation frequency increased with an increasing H_2 concentration from ca. 0.13 h^{-1} at 0.14% H_2 to ca. 1.5 h^{-1} at 1.0% H_2, and (ii) the amplitude of oscillation decreased with an increase of H_2 concentration from ca. 500 ppm NO_x at 0.14% H_2 to 40 ppm NO_x at 1.0% H_2.

Part of the oscillation is shown in Fig. 3 to correlate with NO/H_2 conversions as well as product selectivities at each position (I–V) in the profile. The steady-state (nonoscillatory) NO_x conversion of 73% with H_2 conversion of 100% and N_2 selectivity of 51%, which were obtained after 10 h

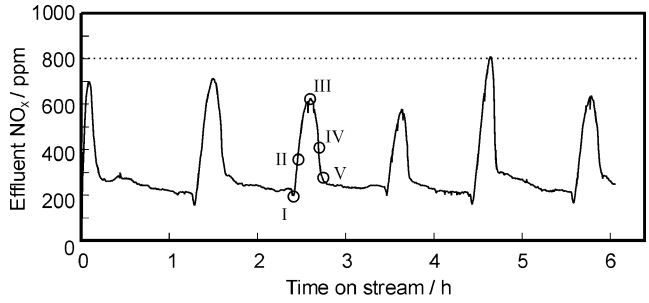

	NO conversion (%)	Selectivity (%)		H_2 conversion (%)
		N_2	N_2O	
Control	72.7	51	49	100.0
I	73.9	152	38	77.2
II	54.0	150	65	60.0
III	23.6	151	112	53.6
IV	48.0	62	105	86.0
V	63.3	44	57	100.0

Fig. 3. Part of oscillation profiles in NO–H_2–O_2 reactions at 90 °C: 0.08% NO, 0.28% H_2, 10% O_2, He balance, W/F = 0.24 s g cm^{-3}. NO/H_2 conversions and N_2/N_2O selectivities at each point are shown in the table.

of reaction (Fig. 1), is used as a control. At the beginning point of the oscillation (I), the conversion of NO was kept at the same level, whereas that of H_2 decreased to 77%. More noticeable is that the N_2 selectivity was far beyond the reaction stoichiometry. With the progression of oscillations to (II) and (III), the NO conversion as well as H_2 conversion continued to decrease and the product selectivity to N_2/N_2O was still higher than the stoichiometry. After this, the NO/H_2 conversions began to increase (IV) and, finally, the original activity and product selectivity close to the steady state were restored at the end of one oscillation cycle (V).

3.2. *NO adsorption property of Pt/TiO_2–ZrO_2*

As was revealed in our previous paper, the present TiO_2–ZrO_2 binary oxide contained base sites available for the oxidative adsorption of NO in the presence of O_2. The adsorbed NO_x is thus considered to be trapped on the base site formed in the porous noncrystalline structure. The formation of excess N_2/N_2O during oscillation (Fig. 3) may imply that NO_x accumulated during the induction period takes part in the reaction with hydrogen. This is consistent with the fact that the oscillation was not observed for NO–H_2–O_2 reaction over Pt supported on SiO_2 and Al_2O_3, the NO_x adsorbability of which is far less than that of TiO_2–ZrO_2.

Adsorptive NO_x uptake of Pt-loaded and unloaded TiO_2–ZrO_2 was evaluated in a flow reactor. Fig. 4 depicts NO breakthrough curves measured in a stream of 0.08% NO, 10% O_2, and He balance at 90 °C. On supplying the gas mixture, the effluent NO_x increased gradually because of removal by adsorption onto TiO_2–ZrO_2. Both samples were nearly saturated with NO_x within an hour, but a slow adsorptive uptake lasted even after 10 h. The initial rate of adsorption was higher for the Pt-loaded than for unloaded

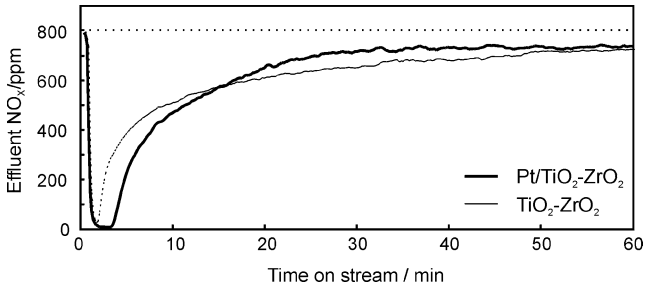

Fig. 4. Breakthrough curves of NO at 90 °C: 0.08% NO, 10% O_2, He balance, W/F = 0.24 s g cm^{-3}.

TiO_2–ZrO_2. Since NO adsorption onto both samples yielded nitrate (NO_3) as evident from parallel in situ DRIFTS measurement, such oxidative adsorption should be facilitated in the presence of Pt. However, the cumulative NO uptakes after 10 h, which was calculated from each breakthrough curves are almost same (ca. 0.4 mmol g^{-1}).

To confirm the role of accumulated NO_x on the catalyst, the response to the reaction transients was evaluated during the oscillation reaction. In this experiment, the standard gas feed, containing 0.08% NO, 0.28% H_2, 10% O_2, and He balance, was switched to a mixture of 0.28% H_2, 10% O_2, and He balance immediately after the beginning of oscillation as shown in Fig. 5a. Nevertheless, the NO_x concentration at the outlet of the catalyst bed did not readily approach to zero. This is evidence of the gradual liberation of adsorbed NO_x from the catalyst to the effluent gas. When the gas supply was returned to the initial NO mixture in a few minutes, the oscillation was soon continued as before. Fig. 5b shows the result for the similar response with longer exposure (ca. 70 min) to the H_2/O_2/He flow, which did not exhibit oscillation even after switching back to the initial NO gas feed. This is probably due to the gradual removal of accumulated NO_x by reaction with H_2 in flowing H_2/O_2/He mixtures. The amount of NO_x adsorbed on the catalyst is therefore considered to determine when the oscillation would set in. The oscillation behavior disappeared when the catalyst after use was treated in a stream of 5% H_2/He at 400 °C. In this case, it took about more than 20 h to initiate the oscillation again.

3.3. NO_x–TPD from catalyst under oscillation

In order to obtain direct evidence of the relation between oscillation and accumulation of NO_x, we next conducted TPD measurements for the 1 wt% Pt/TiO_2–ZrO_2 catalyst under oscillation. The catalyst reaching four different points (I, II, III, and V) in Fig. 3 was quenched immediately to room temperature in He. This is followed by TPD measurement in a stream of He at heating rate of 10 °C min^{-1}. The observed NO_x desorption profiles are shown as a function of temperature in Fig. 6a. Two desorption peaks, denoted to α and β, were observed in the range of 200–400 °C with different desorption temperatures and intensities depending on the position in the oscillation profile (Fig. 3). The characteristic features of these desorption profiles for each points can be summarized as follows: (i) The total amount of accumulated (desorbed) NO_x decreased in the order, I (0.41 mmol g^{-1}) > II (0.38) > III (0.36) > V (0.28). (ii) The area of α-peak decreased from II to III, whereas the area of β-peak decreased from III to V. (iii) Both peaks were shifted toward higher temperatures from I to III, and then returned to the original temperature for V.

For comparison, NO_x–TPD for Pt-unloaded TiO_2–ZrO_2 was measured after exposure to a stream of 0.08% NO, 0.28% H_2, 10% O_2, and He balance at 90 °C for 10 h (Fig. 6b). Interestingly, although the total NO uptake, 0.40 mmol g^{-1} was almost the same as that for Pt-loaded catalyst at point (I) in the oscillation profile (Fig. 3), the desorption profile was completely deferent; i.e., a broad desorption appeared at a higher temperature of ca. 430 °C. This is a clear indication the Pt would play a key role not only in the oxidative NO adsorption but also in the desorption of NO_x in a heating course.

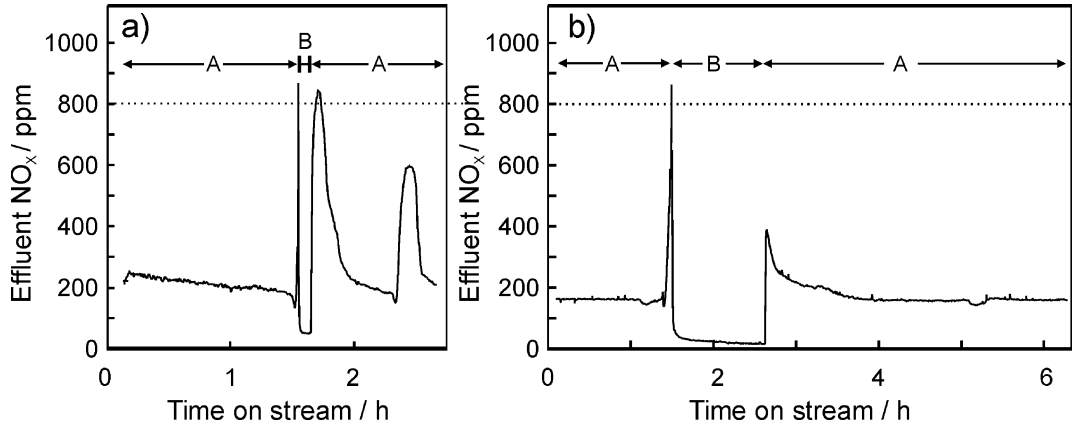

Fig. 5. Response to NO-concentration transients in the oscillating NO–H_2–O_2 reaction: A, 0.08% NO, 0.28% H_2, 10% O_2, He balance, W/F = 0.24 s g cm^{-3}; B, 0.28% H_2, 10% O_2, He balance, W/F = 0.24 s g cm^{-3}.

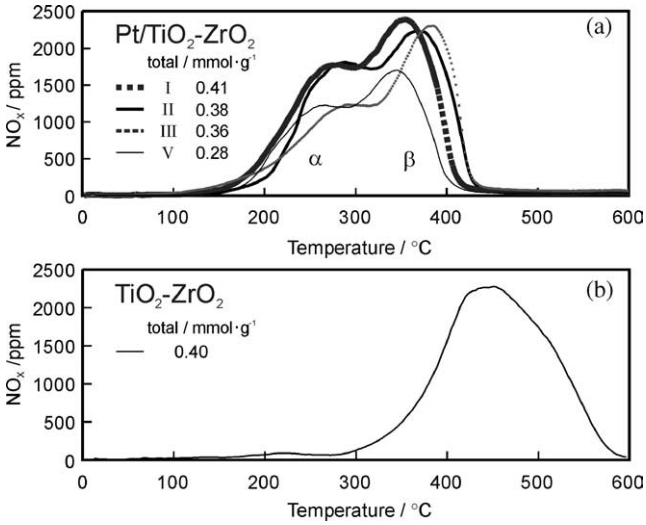

Fig. 6. (a) NO_x–TPD for Pt/TiO_2–ZrO_2 showing oscillation behavior in Fig. 3. I–V, points shown in Fig. 3. (b) NO–TPD for unloaded TiO_2–ZrO_2: TPD in a He flow, 10 °C min^{-1}.

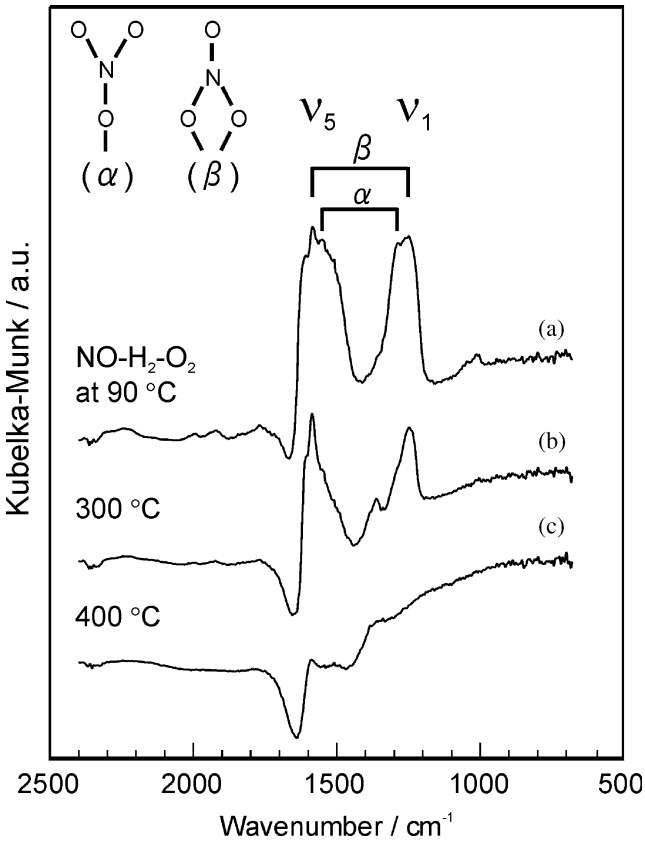

Fig. 7. In situ DRIFT spectra of nitrate formed on Pt/TiO_2–ZrO_2. The spectra were taken after (a) exposing to 0.08% NO, 10% O_2, 0.28% H_2/He at 90 °C and after heating at (b) 300 °C and (c) 400 °C in He.

3.4. *In situ DRIFT for two different NO_x species*

Spectral change in a course of thermal desorption was studied by means of in situ DRIFTS as shown in Fig. 7. On exposure to the reaction mixture (0.08% NO, 0.28% H_2, 10% O_2, and He balance) at 90 °C, two strong bands ascribable to different N–O stretching modes (ν_5 and ν_1) of nitrate (NO_3) appeared on the Pt/TiO_2–ZrO_2 catalyst. All these assignments of observed bands are consistent with those reported previously [21–26]. Each band consists of at least two different components. Generally, the structure of nitrate ligand can be judged from the separation of these two bands; i.e., the separation becomes larger for the bidentate rather than for the unidentate coordinations as summarized by Nakamura [21]. On the basis of the difference of two wavenumbers, $\nu_5 - \nu_1$, the present spectra can be assigned to unidentate ($\nu_5 - \nu_1 \approx 250$ cm^{-1}) and bidentate ($\nu_5 - \nu_1 \approx 340$ cm^{-1}) nitrates. When the catalyst was heated in a flowing He, the unidentate bands were only weakened up to 300 °C. Further heating up to 400 °C led to the disappearance of bidentate bands. Therefore, α and β peaks in the TPD profiles (Fig. 6a) are assigned to unidentate and bidentate nitrates, respectively. The spectrum of adsorbed NO_x onto Pt-unloaded TiO_2–ZrO_2 was very similar to the Pt–loaded catalyst, suggesting that the nitrate species are formed on the surface of TiO_2–ZrO_2.

Table 1
Surface properties of 1 wt% Pt/TiO_2–ZrO_2

BET surface area	207 m^2 g_{cat}^{-1}
Pt dispersion[a]	0.48
Pt surface area	1.1 m^2 g_{cat}^{-1}
NO adsorption[b]	0.41 mmol g_{cat}^{-1}
Surface Ti [c]	1 mmol g_{cat}^{-1}

[a] Determined by O_2–H_2 titration at room temperature.
[b] Determined by measuring a breakthrough curve at 90 °C, 0.08% NO, 10% O_2, and He balance.
[c] The amount of surface Ti averaged on (100) and (001) planes of TiO_2 on the assumption of surface Ti/Zr ratio equal to unity.

4. Discussion

The characteristic of the present TiO_2–ZrO_2 support is a noncrystalline porous structure having hetero-junctions at the boundary of the two oxide components, where zirconium ions act like a Lewis acid, and titanium ions as a base [11,12]. The base site appears to be essential to the large NO adsorption, which is promoted by the platinum catalyst. Table 1 shows characteristic parameters concerning adsorption onto TiO_2–ZrO_2. The NO uptake per unit catalyst weight is 0.41 mmol g^{-1} as was evident from Fig. 4. The Pt surface area on 1 wt% Pt/TiO_2–ZrO_2 was very small compared to the total surface area, 207 m^2 g^{-1}. Almost all NO uptake for 1 wt% Pt/TiO_2–ZrO_2 is therefore ascribable to the adsorption onto the TiO_2–ZrO_2 support. Assuming the Ti/Zr ratio on the surface to be unity, it is suggested that ca. 40% of Ti sites exposed on the surface are occupied by NO_x.

Considering the NO adsorption property together with TPD and DRIFTS experiments, a possible reaction scheme for the oscillatory NO–H_2–O_2 reaction over Pt/TiO_2–ZrO_2 can be depicted as in Fig. 8. The roman numerals in Fig. 8

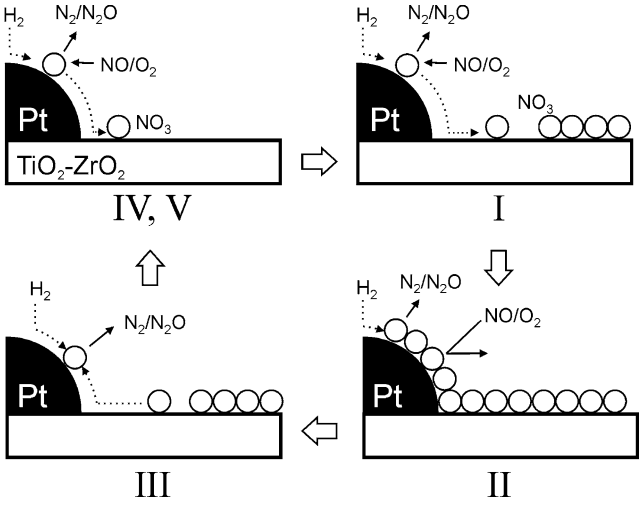

Fig. 8. A possible model for kinetic rate oscillation over $Pt/TiO_2–ZrO_2$.

corresponding to those in Fig. 3 represent some characteristic steps in the present oscillating reaction. In a reaction atmosphere at low temperatures $\leqslant 100\,^{\circ}C$, NO is adsorbed onto the Pt surface as nitrate. This severely limits simple $H_2–O_2$ combustion, so that the minimum hindrance of the $NO_x–H_2$ reaction from an excess O_2 can be attained. Parallel to this catalytic reaction, part of NO adsorbed would be spilled over onto the $TiO_2–ZrO_2$ support to yield unidentate and bidentate nitrates on the base site (I). With progression of this NO_x spillover, incremental amounts of nitrate were accumulated to monopolize the surface of the support (I, II). Above certain coverage of the support and Pt with nitrate, the strong inhibition of NO adsorption would cause a significant decrease of $NO_x–H_2$ reaction rate (II). During this deactivation process, however, the reactions between accumulated nitrates and hydrogen over Pt would continuously consume nitrates supplied by back-spillover (III), which in turn leads to the decrease of the NO coverage on the support. This is the reason why N_2/N_2O exceeding the reaction stoichiometry was formed in these steps. Finally, the oxidative NO adsorption and subsequent reaction with hydrogen would restart over Pt to enter into a new oscillation cycle (V).

One may consider that the induction period before the onset of oscillation, ca. 20 h (Fig. 1), seems like a long time for the process from (I) to (II), because the adsorptive NO uptake onto $TiO_2–ZrO_2$ was nearly saturated within an hour (Fig. 4). Actually, however, oxidative NO uptake in the $NO–H_2–O_2$ mixture would take a longer time to be saturated, compared to in the $NO–O_2$ mixture, due to a competitive $NO_x–H_2$ reaction over Pt. This is a reason why a longer induction period is observed at higher H_2 concentration in the gas feed. As was observed in Fig. 2, the oscillation frequency and amplitude are also sensitive to the concentration of H_2. This effect appears to be associated with the stability of accumulated nitrate. At low concentrations of H_2, the nitrate adsorbed around Pt is so stable that a large amount of accumulation is possible on the support. This will result in a low-frequency oscillation cycle with a significant drop of catalytic activity. By contrast, an incremental concentration of H_2 decreases the stability of nitrate, leading to more frequent cycles between the saturation of adsorption and subsequent removal by H_2. Also, since the NO_x reduction proceeds more rapidly at higher H_2 concentration, the oscillation amplitude should become less intense.

The shift of NO_x desorption temperatures (Fig. 6a) from (I) to (V) during oscillation should also be explained on the proposed mechanism. Judging from a comparison of Fig. 6a and b, platinum clearly promotes the desorption of nitrate as NO_x from the $TiO_2–ZrO_2$ support. Nitrate on the support would back-spillover onto Pt, which plays a role of a take-off point to a gas phase. This effect gives a reason why two desorption peaks, α and β, were shifted toward higher temperatures when the oscillation proceeds from (I) to (III). The thermal desorption should occur first for the nitrates on Pt and subsequently for those on $TiO_2–ZrO_2$ in the vicinity of Pt, but higher temperatures would be required for those on $TiO_2–ZrO_2$ distant from Pt. During the oscillation process from (I) to (III), the removal of nitrate by the reaction with H_2 should be spread in a similar manner, from Pt to far out over the support, leading to a shift of desorption temperature. After removing nitrate around Pt by reaction with H_2 and restoring the initial steady-state activity (V), the adsorption increases the number of nitrate in the vicinity of Pt, leading to the decrease of temperature for the NO desorption.

The oscillation in the present system is useful for understanding the mechanism of $NO–H_2–O_2$ reactions over Pt supported on NO_x-adsorbing support. However, as in other catalytic processes, the occurrence of oscillation is not desirable from practical points of view. Further research is necessary for designing novel NO_x-adsorbing support materials, which enable the precise control of Lewis-base sites.

5. Conclusion

The following conclusions have emerged from this study.

1. The $Pt/TiO_2–ZrO_2$ catalyst exhibited oscillations in the $NO–H_2–O_2$ reactions at $90\,^{\circ}C$, which is typical for the support having a large amount of NO_x adsorption. The oscillations yielded more N_2/N_2O than expected from the NO conversion, suggesting that the NO_x species accumulated on the support would take part in the catalytic reaction.
2. The accumulation of NO_x proceeded via the oxidative adsorption of NO as unidentate and bidentate nitrates (NO_3) on the surface of $TiO_2–ZrO_2$, which was promoted by Pt in the presence of O_2. The bidentate nitrate was more strongly bound to the support in comparison to the unidentate nitrate.
3. At a certain point approaching to the saturation of adsorption, the oxidative NO adsorption would be inhib-

ited so that the NO conversion is steeply dropped. However, the reaction between H_2 and accumulated nitrate decreases the surface coverage of nitrate to restart the catalytic NO–H_2–O_2 reaction over Pt.

Acknowledgments

The present study was financially supported by the New Energy and Industrial Technology Development Organization (NEDO)/Research Institute of Innovative Technology for Earth (RITE) and Grant-in-Aid for Scientific Research from the Ministry of Education, Sports, and Culture.

References

[1] K. Yokota, M. Fukui, T. Tanaka, Appl. Surf. Catal. 121/122 (1997) 273.
[2] B. Frank, G. Emig, A. Renken, Appl. Catal. B 19 (1998) 45.
[3] A. Ueda, A. Nakato, M. Azuma, T. Kobayashi, Catal. Today 45 (1998) 135.
[4] R. Burch, M.D. Coleman, Appl. Catal. B 23 (1999) 115.
[5] R. Burch, A.A. Shestov, J.A. Sullivan, J. Catal. 188 (1999) 69.
[6] M. Machida, S. Ikeda, D. Kurogi, T. Kijima, Appl. Catal. B 35 (2001) 107.
[7] C.N. Costa, V.N. Stathopoulos, V.C. Belessi, A.M. Efstathiou, J. Catal. 197 (2001) 350.
[8] R. Burch, M.D. Coleman, J. Catal. 208 (2002) 435.
[9] M. Machida, T. Watanabe, S. Ikeda, T. Kijima, Catal. Commun. 3 (2002) 233.
[10] M. Machida, S. Ikeda, T. Kijima, Stud. Surf. Sci. Catal. 145 (2003) 243.
[11] K. Arata, S. Akutagawa, K. Tanabe, Bull. Chem. Soc. Jpn. 49 (1976) 390.
[12] K. Arata, K. Tanabe, Bull. Chem. Soc. Jpn. 53 (1980) 299.
[13] L.F. Razon, R.A. Schmitz, Catal. Rev.-Sci. Eng. 28 (1986) 89.
[14] U.S. Ozkan, M.W. Kumthekar, G. Karakas, J. Catal. 171 (1997) 67.
[15] B.K. Cho, J.E. Yie, K.M. Rahmoeller, J. Catal. 157 (1995) 14.
[16] G. Centi, L. Dall'Olio, S. Perathoner, J. Catal. 192 (2000) 224.
[17] E.M. El-Malki, R.A. van Santen, W.M.H. Sachtler, J. Catal. 196 (2000) 212.
[18] C.A. de Wolf, B.E. Nieuwenhuys, Catal. Today 70 (2001) 287.
[19] F.V. Caballero, L. Viente, Chem. Eng. Sci. 58 (2003) 5087.
[20] M. Machida, D. Kurogi, T. Kijima, J. Phys. Chem. B 107 (2003) 196.
[21] K. Nakamoto, Infrared and Raman Spectra of Inorganic and Coordination Compounds, fourth ed., Wiley, New York, 1986.
[22] B. Klingenberg, M.A. Vannice, Appl. Catal. B 21 (1999) 19.
[23] S.J. Huang, A.B. Walters, M.A. Vannice, Appl. Catal. B 26 (2000) 101.
[24] F.C. Meunier, V. Zuzaniuk, J.P. Breen, M. Olsson, J.R.H. Ross, Catal. Today 59 (2000) 287.
[25] A. Martinez-Arias, J. Soria, J.C. Consesa, X.L. Seoane, A. Arcoya, R. Cataluna, J. Chem. Soc., Faraday Trans. 91 (1995) 1679.
[26] M. Machida, M. Uto, D. Kurogi, T. Kijima, J. Mater. Chem. 11 (2001) 900.